11th World Congress on Computational Mechanics (WCCM XI)
5th European Conference on Computational Mechanics (ECCM V)
6th European Conference on Computational Fluid Dynamics (ECFD VI)
E. Oñate, J. Oliver and A. Huerta (Eds)

DYNAMIC WALL MODELLING FOR LARGE-EDDY SIMULATIONS. APPLICATION TO HIGH REYNOLDS NUMBER AERODYNAMICS OF COMPLEX GEOMETRIES.

CALAFELL J.[*,†], CARMONA A.[*], LEHMKUHL O.[*,†], PÉREZ-SEGARRA C.D.[*] AND OLIVA A.[*]

[*] Heat and Mass Transfer Technological Center
Polytechnical University of Catalonia (UPC)
Colom 11, 08222, Terrassa (Barcelona) Spain
e-mail: cttc@cttc.upc.edu, web page: http://www.cttc.upc.edu

[†]Termo Fluids, S.L.
Avda. Jaquard, 97 1-E, 08222 Terrassa (Barcelona) Spain
e-mail: termofluids@termofluids.com, web page: http://www.termofluids.com

Key words: Boundary Layer, Dynamic Wall Model, Large Eddy Simulation, Aerodynamics, Unstructured mesh, Ahmed Car.

Abstract. Nowadays, Large Eddy Simulations (LES) calculations are still prohibitively expensive at high Reynolds Number, specially for aerodynamic applications where wall flows are present. Different strategies can be found in the literature in order to reduce mesh requirements at the near-wall region such as hybrid Reynolds Averaged Navier Stokes (RANS)/LES approach or Wall Functions. Dynamic wall models in which this paper is focused, are part of these strategies. The present model is intended to make feasible calculations of industrial applications that are computationally prohibitive until now. Since complex geometries are found in most of these applications, the model has been formulated for unstructured meshes. In order to validate the mathematical formulation and evaluate the model performance, two diferent tests have been computed. Firstly, a very unresolved Channel Flow case at $Re = 1 \times 10^5$ or $Re_\tau = 2260$ is solved. Afterwards, the model is also tested with the Ahmed Car case, that from the flow physics point of view is more complex than the Channel Flow, including flow features as boundary layer detachment and recirculations. Numerical results are presented in comparison with experimental ones for both cases.

1 Introduction

At present, Large Eddy Simulations (LES) calculations are still prohibitively expensive for most of the industrial applications. This is because most of the industrial flows occur in

large domains at high Reynolds Number and usually, extensive wall areas are present. All these characteristics increase the flow complexity, and therefore the mesh requirements. In order to reduce the required grid size at the near-wall region, different strategies can be found in the literature such as hybrid Reynolds Averaged Navier Stokes (RANS)/LES approach or Wall Functions. This paper is focused in dynamic wall models which are part of the methodologies that are being developed to lower computational requirements in the wall domain. The present model is intended to make feasible calculations of industrial applications that are computationally prohibitive until now. That is why the model has been developed for unstructured meshes since complex geometries are found in most of the industrial applications of interest.

In order to validate the mathematical and numerical formulation, a very unresolved Channel Flow case at $Re = 1 \times 10^5$ equivalent to $Re_\tau = 2260$ is solved. The numerical results provided by the wall model are compared with the mean velocity profile in the stream-wise direction also known as the wall law. This way, it will be checked if the model reproduces the real phyisics of the boundary layer region. Afterwards, the model performance is evaluated by measuring the improvement of the numerical results in the whole LES domain caused by the use of the wall model in two different cases. To do this, the LES results of the Channel Flow are used along with the results of an Ahmed Car test at $Re = 7 \times 10^5$. The case of the Ahmed Car include more complex flow features than the channel flow such as boundary layer detachment and flow recirculations. Experimental results of mean velocity profiles in the recirculation region are provided for this case. Further details of the mathematical and numerical formulation of both, the LES and the wall models are given below.

2 Mathematical and numerical formulation of the LES

The turbulent flow is described by means of LES using symmetry-preserving discretizations. The spatial filtered and discretized Navier-Stokes equations can be written as,

$$\mathsf{M}\boldsymbol{u} = 0 \tag{1}$$

$$\Omega\frac{\partial\overline{\boldsymbol{u}}}{\partial t} + \mathsf{C}\left(\overline{\boldsymbol{u}}\right)\overline{\boldsymbol{u}} + \nu\mathsf{D}\overline{\boldsymbol{u}} + \rho^{-1}\Omega\mathsf{G}\overline{\boldsymbol{p}} \;=\; \mathsf{C}\left(\overline{\boldsymbol{u}}\right)\overline{\boldsymbol{u}} - \overline{\mathsf{C}\left(\boldsymbol{u}\right)\boldsymbol{u}} \;\approx\; -\mathcal{M}\mathcal{T}_m \tag{2}$$

where M, C, D and G are the divergence, convective, diffusive and gradient operators, respectively, Ω is a diagonal matrix with the sizes of control volumes, ρ is the fluid density, ν the viscosity, $\overline{\boldsymbol{p}}$ represents the filtered pressure, $\overline{\boldsymbol{u}}$ is the filtered velocity, $\mathcal{M}$ represents the divergence operator of a tensor, and $\mathcal{T}_m$ is the SGS stress tensor, which is defined as,

$$\mathcal{T}_m = -2\nu_{sgs}\overline{\mathcal{S}} + (\mathcal{T}_m : \mathsf{I})\mathsf{I}/3 \tag{3}$$

where $\overline{\mathcal{S}} = \frac{1}{2}[\mathsf{G}(\overline{\boldsymbol{u}}) + \mathsf{G}^*(\overline{\boldsymbol{u}})]$. To close the formulation, a suitable expression for the SGS viscosity, ν_{sgs}, must be introduced. In the present work the WALE model [1] within a

variational multiscale framework [2] (VMS-WALE) and the Smagorinsky model have been used initially for the Channel Flow case. For the Ahmed Car test, the standard WALE model has been applied. Regarding the VMS stategy, it was originally formulated for the Smagorinsky model by Huges in the Fourier space. However, in our implementation, the formulation is closed by means the WALE model as described below. In the variational multiscale (VMS) approach, three classes of scales are considered: large, small and unresolved scales. If a second filter with filter length $\hat{l}$ is introduced (usually called test filter), a splitting of the scales can be performed, $f^{'} = \overline{f} - \hat{f}$. Following Vreman notation [3], $f^{'}$ is called the small-scale component, $\hat{f}$ the large-scale component and $\overline{f}$ is the original resolved quantity. Thus, for the large-scale parts of the resolved $\overline{\boldsymbol{u}}$ a general governing equation can be derived,

$$\Omega\frac{\partial\overline{\boldsymbol{u}}}{\partial t} + \mathsf{C}\left(\overline{\boldsymbol{u}}\right)\overline{\boldsymbol{u}} + \nu\mathsf{D}\overline{\boldsymbol{u}} + \rho^{-1}\Omega\mathsf{G}\overline{\boldsymbol{p}} \;=\; -\frac{\partial\widehat{\mathcal{T}}}{\partial x_j} - \frac{\partial\mathcal{T}^{'}}{\partial x_j} \tag{4}$$

Inspecting equation 4 it is possible to identify $\widehat{\mathcal{T}}$ as the subgrid term in the large-scale equation and $\mathcal{T}^{'}$ as the subgrid small-scale term. Now, neglecting the effect of unresolved scales in the large-scale equation ($\widehat{\mathcal{T}} \approx 0$) , we only need to model the $\mathcal{T}^{'}$. In our implementation the *small-small* strategy is used in conjunction with the WALE model:

$$\begin{aligned}
\mathcal{T}^{'} &= -2\nu_{sgs}\mathcal{S}_{\mathsf{ij}}{}^{'} + \frac{1}{3}\mathcal{T}^{'}\delta_{ij} \\
\nu_{sgs} &= (C_w^{vms}\Delta)^2\frac{(\mathcal{V}_{\mathsf{ij}}{}^{'} : \mathcal{V}_{\mathsf{ij}}{}^{'})^{\frac{3}{2}}}{(\mathcal{S}_{\mathsf{ij}}{}^{'} : \mathcal{S}_{\mathsf{ij}}{}^{'})^{\frac{5}{2}} + (\mathcal{V}_{\mathsf{ij}}{}^{'} : \mathcal{V}_{\mathsf{ij}}{}^{'})^{\frac{5}{4}}} \\
\mathcal{S}_{\mathsf{ij}}{}^{'} &= \frac{1}{2}[\mathsf{G}(\overline{\boldsymbol{u}^{'}}) + \mathsf{G}^{*}(\overline{\boldsymbol{u}^{'}})] \\
\mathcal{V}_{\mathsf{ij}}{}^{'} &= \frac{1}{2}[\mathsf{G}(\overline{\boldsymbol{u}^{'}})^2 + \mathsf{G}^{*}(\overline{\boldsymbol{u}^{'}})^2] - \frac{1}{3}(\mathsf{G}(\overline{\boldsymbol{u}^{'}})^2\mathsf{I})
\end{aligned} \tag{5}$$

where C_w^{vms} is the equivalent of the WALE coefficient for the *small-small* VMS approach and in the finite volume context its value lies in the range between 0.3 and 0.5. In our studies a value of 0.325 is used.

The governing equations have been discretized on a collocated unstructured grid arrangement by means of second-order spectro-consistent schemes [4]. Such schemes are conservative, i.e. they preserve the symmetry properties of the continuous differential operators and ensure both, stability and conservation of the kinetic-energy balance even at high Reynolds numbers and with coarse grids. i.e. they preserve the kinetic energy equation. These conservation properties are held if, and only if the discrete convective operator is skew-symmetric ($\mathsf{C}\left(\boldsymbol{u}\right) = -\mathsf{C}^{*}\left(\boldsymbol{u}\right)$), the negative conjugate transpose of the discrete gradient operator is exactly equal to the divergence operator ($-\left(\Omega\mathsf{G}\right)^{*} = \mathsf{M}$) and the diffusive operator D, is symmetric and positive-definite. For the temporal discretization of the momentum equation a two-step linear explicit scheme on a fractional-step

method has been used for the convective and diffusive terms, while for the pressure gradient term an implicit first-order scheme has been used. This methodology has been previously used with accurate results for solving the flow over bluff bodies with massive separation [5, 6, 7].

3 The Dyamic Wall Model

The dynamic wall model (DWM) is based on the implicit resolution of the full spatial discretized RANS equations (6) in a fine embedded mesh called wall domain mesh (WDM). The WDM is generated by extrusion of the superficial mesh of the solid face between the wall and the first off-wall node of the LES mesh (LDM) [8].

$$\Omega \frac{\partial \langle \boldsymbol{u} \rangle}{\partial t} + \mathsf{C}\left(\langle \boldsymbol{u} \rangle\right) \langle \boldsymbol{u} \rangle = \mathcal{M}\left[2\left(\nu + \nu_T\right) \langle \mathcal{S} \rangle\right] - \rho^{-1} \Omega \mathsf{G} \langle \boldsymbol{p} \rangle \tag{6}$$

M, C and G are the divergence, convective, and gradient operators respectively, $\langle \mathcal{S} \rangle$ is the mean strain rate tensor, Ω is a diagonal matrix with the sizes of control volumes, ρ is the fluid density, ν the viscosity, ν_T the turbulent RANS viscosity and finally, $\langle \boldsymbol{p} \rangle$ and $\langle \boldsymbol{u} \rangle$ the time averaged pressure and velocity respectively.

The equations are solved numerically by means the finite volume method. Symmetry preserving numerical schemes have been used to carry out the spatial discretization of the convective term, while second order central difference scheme has been applied for the diffusive one. In order to solve the velocity-pressure coupling, an implicit projection method has been implemented.

Regarding the boundary conditions, Dirichlet ones are prescribed at the outer surface for velocities and pressure taking its values from the LES domain, while at the solid face, no-slip and Neumann conditions are applied for velocities and pressure respectively. Finally, if side boundaries do exist, the same boundary conditions than LES domain are applied to them. In figure 1, the WDM geometry is shown.

The RANS equations turbulent eddy viscosity (ν_T) is obtained according the Spalart-Allmaras model, a one-equation RANS model suitable for wall bounded flows [9].
Once the mean velocity field is obtained, an accurate mean wall shear stress can be computed according the following expression:

$$\tau_{wi} \approx (\mu + \mu_T) \frac{u_{iy1}}{\delta_{y_1}} \tag{7}$$

Where τ_{wi} is the i^{th} component of the shear stress related to a local coordinate system parallel to the solid surface ij, μ is the local viscosity, μ_T is the local turbulent viscosity, u_{iy1} is the i^{th} component of the velocity corresponding to the first off-wall node of the WDM, and δ_{y_1} is the distance between the node and the wall. The calculated value is used to feed the global LES calculation as a boundary condition through the diffusive term.

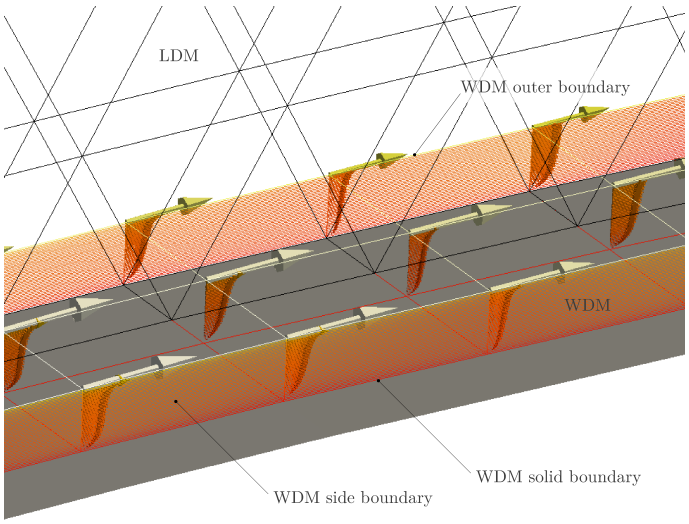

Figure 1: Dynamic wall model scheme. The WDM is embedded into the LDM.

The main advantage of this methodology arises from the fact that the explicit LES-domain mesh is much coarser than the implicit RANS/wall-domain one. Hence, a much bigger time step can be used compared to the one that should be taken if the LDM size were of the same order of magnitude than the WDM one.

4 Mathematical formulation validation and model performance evaluation: The Channel Flow test.

The main objective of this section is not to obtain a very well resolved Channel Flow but to check if the wall model reproduces the real boundary layer physics and to evaluate if the model is able to compute a correct value of wall shear stress (τ_{wi}). The effects of the new value of τ_{wi} on the overall LES results are also checked. To do so, a very coarse mesh of 68x33x34 control volumes has been used as shown in figure 2. Periodic conditions have been prescribed in all directions except in the upper and lower walls, where solid wall conditions are set. Two different turbulence models have been used for the LES domain, the VMS-WALE and the Smagorinsky one. In cases where the dynamic wall model has been used, the WDM has been extruded in 50 layers.

A high Reynolds number of $Re = 1 \times 10^5$ has been selected in order to challenge the wall model. This Reynolds number is defined as $Re = 2\delta\overline{U}/\nu$ where δ is the channel half height, $\overline{U}$ is the bulk velocity, and ν is the kinematic viscosity of the fluid. According the empirical expression $Re_\tau = 0.09Re^{0.88}$ [10] this value of Re is equivalent to $Re_\tau = 2260$.

From general turbulence theory, an expression derived from the stream-wise mean momentum equation, states that the wall shear stress and the pressure gradient in the

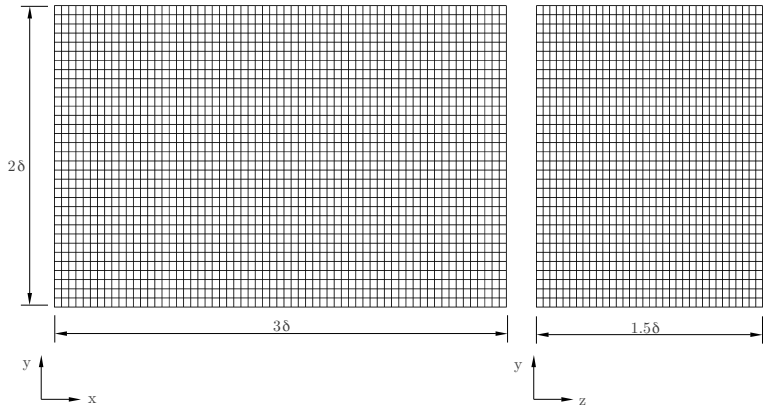

Figure 2: Channel Flow LES domain mesh.

flow direction are related as follows [10]:

$$-\frac{dp_w}{dx} = \frac{\tau_w}{\delta} \tag{8}$$

In order to check if the model is able to compute an accurate wall shear stress, the strategy is based on prescribing a calculated pressure gradient from the Re_τ by using equation 8 and checking if the calculated numerical value of Re_τ matches the value initially used to determine the imposed pressure gradient. If so, we can conclude that the numerical solution matches the analytic one as Re_τ is a direct function of τ_w, and therefore that the model is able to compute an accurate wall shear stress. In table 1, the Re_τ calculated by using and not using the DWM, are compared with the expected value (the one used to evaluate dp_w/dx).

Finally, in order to check the improvement of the numerical results of the LES domain, the values obtained with the dynamic wall model and those obtained without it, will be compared. On the other hand, it will be analyzed if the computed mean velocity profiles matches the law of the wall. This law describes the mean velocity profile in the flow direction as a function of the distance to the wall [10]: $u^+ = y^+$ if $y^+ < 5$ (i.e. the viscous sublayer) and $u^+ = (1/\kappa)\ln y^+ + B$ if $y^+ > 30$ (i.e. the log-law region). The superindex $^+$ denotes that the variable is in wall units while u^+ is the stream-wise mean velocity, y^+ is the wall distance, k is the von Kármán constant ($k = 0.41$), and B is a constant whose value for the channel flow is $B = 5.2$.

As a measure of the mesh coarseness, at $Re_\tau = 2260.6$ the first off-wall node of the LDM is located at $y^+ = 68.506$, it is far above the viscous sublayer and well into the logarithmic law region.

4.1 The Channel Flow test results.

In table 1 a comparison between the reference values of Re_τ and the calculated numerical results is shown. The numerical results have been obtained with and without wall model in order to check the model improvements to the Re_τ evaluation. Regarding the LES domain, two different LES models have been used in order to evaluate the interaction between the dynamic wall and the LES. In the present work, the Smagorinsky and the VMS-WALE have been used.

Table 1: Comparison between the reference Re_τ value, and the numerical results calculated with and without the dynamic wall model by means two different LES models.

LES model	ref. Re_τ	Re_τ w/o model	rel. err. [%]	Re_τ w/ model	rel. err. [%]
Smagorinsky	2260.6	2301.0	1.81	2241.4	0.84
VMS-WALE	2260.6	2081.0	7.94	2244.1	0.72

Regarding the mean velocity profiles, in figures 3.a and 3.b, the mean stream-wise velocity component is plotted in wall units as a function of the wall distance that is represented in logarithmic scale. Numerical results obtained with the VMS-WALE and the Smagorinsky models are displayed in figures 3.a and 3.b respectively. For both LES models, computations with and without dynamic wall model have been carried out and plotted. Finally, mean velocity profiles are compared with the law of the wall that is also displayed in the figures. Between $y^+ = 0$ and $y^+ = 5$ the viscous sublayer behavior is plotted while for values higher than $y^+ = 30$ the logarithmic law is shown.

4.2 Conclusions from the Channel Flow test.

While the first off-wall node of the LDM is located at $y^+ = 68.506$, the first node of the WDM is at $y^+ = 0.856$ lying well into the viscous sublayer. The velocity profile in this region is linear and that allows an accurate computation of the wall shear stress as it can be observed in table 1. Errors in the calculation of Re_τ are quite lower when calculated through the wall model for the VMS-WALE case. It has to be taken into account that the objective of these calculations was not to obtain a well resolved Channel Flow. Instead, the main target was to evaluate the improvement of the numerical results with respect to a reference when using the dynamic wall model. Regarding the mean velocity profiles, an improvement in the LES domain is observed, specially in the case of the Smagorinsky model. The numerical results obtained with the DWM fit better to the law of the wall, specially for the first off-wall node of the LDM. Despite the improvement is much significant in the Smagorinsky case, the overall results are better with the VMS-WALE model. On the other hand, when looking at the wall domain results, it is observed that the law of the wall is properly matched in the linear zone (i.e. $y^+ < 5$) in both cases. However, in the log-law region, the results fit slightly better with the VMS-WALE model.

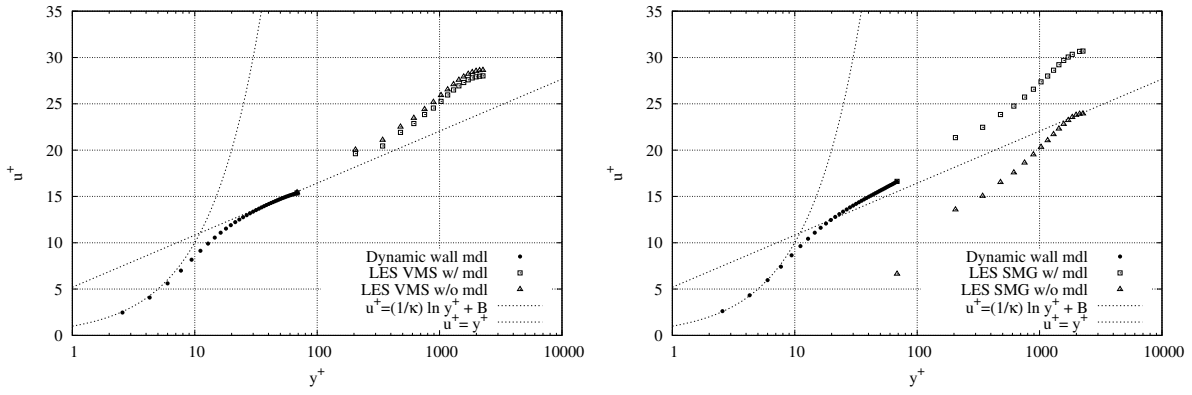

(a) (b)

Figure 3: Mean velocity profiles of the stream-wise velocity component obtained with and without DWM vs. wall distance at $Re_\tau = 2260$. VMS-WALE and Smagorinsky LES models are used to obtain numerical results in figure (a) and (b) respectively . All variables are in wall units and x-axis is represented in logarithmic scale.

These observations leads us to conclude that having a proper LES model is as necessary as having a well resolved near wall zone through the wall model. Despite the significance of the interaction between the wall and the LES models, it is important to remark that in the linear zone the wall law is properly fitted regardless the subgrid model. Taking into account that the shear stress depends only on the velocity profile in this region, that is coherent with the Re_τ values shown in table 1 where the numerical results are quite similar each other and do agree fairly well with reference values for both LES models.

5 The Ahmed Car test.

The standard benchmark case of the Ahmed Car has been computed at Reynolds Number $Re = 7 \times 10^5$, based on the inlet velocity, the vehicle height and the fluid viscosity. The slant angle of the back surface is 25°. The case has been selected because of its complex flow characteristics, including boundary layer detachment and flow recirculations, and the availability of experimental measurements of mean velocity profiles in the recirculation zone. A coarse mesh of 1.7×10^5 control volumes (CV) has been used in order to check the dynamic wall performance. Two cases have been performed, both using the WALE as a subgrid-scale model. In the first one, the dynamic wall model has been used while in the second one, only the LES model has been applied. In the case that uses the wall model, the wall domain mesh is extruded in 40 layers. In figure 4, a snapshot of the LES domain mesh together with the extruded wall domain grid is shown.

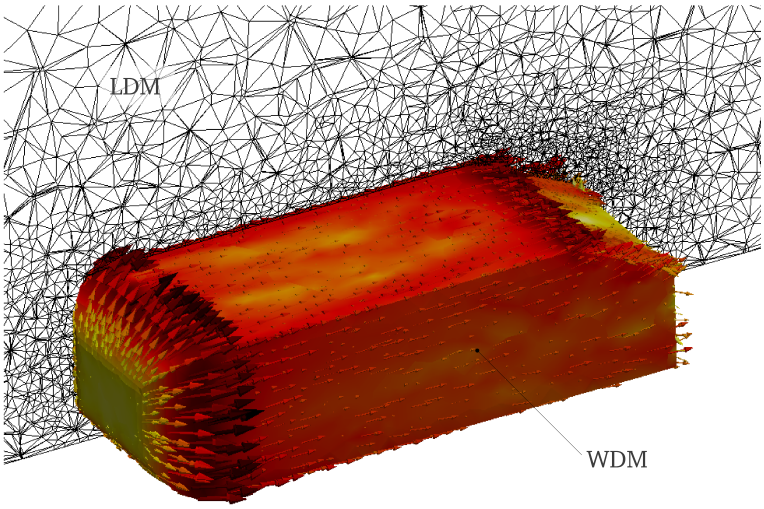

Figure 4: Ahmed Car LES domain mesh together with the wall domain mesh.

5.1 The Ahmed Car test results.

In figure 5.a, the mean velocity profiles obtained with and without the dynamic wall model are shown. These results have been obtained with a mesh of 1.7×10^5 CV. The results are plotted at different stream-wise positions. Finally, numerical results are compared with experimental ones provided by Erlangen University (Nuremberg).

On the other hand, in figure 5.b, the same numerical results obtained with the coarse (with and without wall model) are compared with results obtained by using a finer mesh of 1×10^6 CV [11]. This plot allows us to evaluate the performance of the wall model by comparing the results between two cases with identical meshes but with different wall treatment, and another case that uses a much finer mesh but without wall model.

5.2 Conclusions from the Ahmed Car test.

In the cases performed with the coarse mesh, it can be observed in figure 5.a that the numerical results fit much better the experimental ones when the wall model is working. On the other hand, in figure 5.b, when comparing the coarse mesh results with the fine mesh ones, this improvement is also highlighted. Similar results are obtained in the modeled wall LES with coarse mesh if compared to the ones that have been obtained without wall model but using a six times finer grid. Hence, it can be concluded that in this case, the use of the dynamic wall model causes a significant improvement of the results.

6 General conclusions.

The dynamic wall model has been tested with the reference cases of Channel Flow and Ahmed Car tests of which reference results were available. In both cases it has been

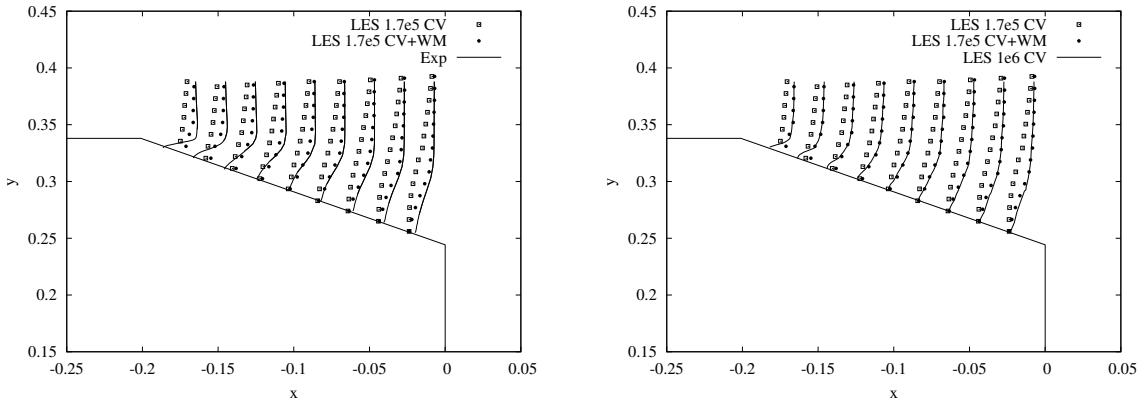

(a) (b)

Figure 5: Comparison between mean velocity profiles obtained with a mesh of 1.7×10^5 CV with and without wall model. In figure (a), numerical results are compared with experimental ones while in figure (b), results are compared with LES data obtained with a mesh of 1×10^6 CV without wall model. All numerical results are computed by means WALE LES model.

proved that the model improves the LES results when using coarse meshes. The results obtained in the Channel Flow case show that it exists an interaction between the wall and the LES models. A proper combination of both models is necessary to obtain good results. However the wall model is able to reproduce the real physics of the boundary layer linear region regardless which subgrid model is used. This is an important observation because it ensures that the model is able to compute a proper shear stress independently of which LES model is used. Regarding the results in the LES domain, in all cases an improvement is observed when using the wall model in coarse meshes. In the case of the Ahmed Car, the results obtained by using a coarse mesh together with the wall model are similar to those obtained by using a six times finer grid. Further studies analyzing the influence of the number of WDM layers will be carried out as well as different combinations of turbulence models both, in the LES and in the WDM-RANS domains.

REFERENCES

[1] Nicoud, F. and Ducros, F. Subgrid-scale stress modelling based on the square of the velocity gradient tensor. *Flow. Turbul. Combust.* (1999) **62**:183-200.

[2] Hughes, T.J.R. Mazzei, L. and Jansen, K.E. Large eddy simulation and the variational multiscale method. *Comput. Vis. Sci.* (2000) **3**:47-59.

[3] Vreman, A.W. The adjoint filter operator in large-eddy simulation of turbulent flow. *Phys. Fluids.* (2004) **16**:2012.

[4] Verstappen, R.W.C.P. and Veldman, A.E.P. Symmetry-preserving discretization of turbulent flow. *J. Comput. Phys.* (2003) **187**:343-368.

[5] Lehmkuhl, O. Rodríguez, I. Baez, A. Oliva, A. and Pérez-Segarra, C.D. On the large-eddy simulations for the flow around aerodynamic profiles using unstructured grids. *Comput. Fluids.* (2013) **84**:176-189.

[6] Lehmkuhl, O. Rodríguez, I. Borrell, R. and Oliva, A. Low-frequency unsteadiness in the vortex formation region of a circular cylinder. *Phys. Fluids.* (2013) **25**:085109.

[7] Rodríguez, I. Borrell, R. Lehmkuhl, O. Prez-Segarra, C.D. and Oliva, A. Direct numerical simulation of the flow over a sphere at Re = 3700 *J. Fluid Mech.* (2011) **679**:263-287.

[8] Wang, M. and Moin, P. Dynamic wall modeling for large-eddy simulation of complex turbulent flows. *Phys. Fluids.* (2002) **14**N7:2043-51.

[9] Spalart, P.R. and Allmaras, S.R. A One-Equation Turbulence Model for Aerodynamic Flows. *Rech. Aerospatiale.* (1944) **1**:5-21.

[10] Pope, S.B. *Turbulent Flows* Cambridge University Press (2000)

[11] Aljure, D.E. Rodríguez, I. Lehmkhul, O. Borrell, R. and Oliva, A. Flow and turbulent structures around simplified car models. *Proc. Conf. on Modelling fluid flow CMFF'12 (Budapest)* (2012) 247-254.